MOFs on Surfaces

DOI: 10.1002/anie.200900378

Growth Mechanism of Metal–Organic Frameworks: Insights into the Nucleation by Employing a Step-by-Step Route**

*Osama Shekhah, Hui Wang, Denise Zacher, Roland A. Fischer, and Christof Wöll**

Metal–organic frameworks (MOFs)[1–4] are an emerging, class of porous materials. MOFs are highly ordered, crystalline coordination polymers of persistent porosity with specific surface areas exceeding that of traditional adsorbents, such as zeolites and active carbons.[1] Whereas initial research on MOFs was mainly driven by the interest to use them as gas-storage (e.g. CH_4, H_2, CO_2) materials,[5] various other applications were proposed and demonstrated, including separation, sensing, catalysis, drug release,[5,6] and the embedding of (metal and metal oxide) nanoparticles.[7–9]

Presently, the search for new types of MOFs is largely by trial-and-error, because very little is known about the details of the MOF crystal growth and nucleation process. In a 2006 review article on MOFs by Cheetham et al. it was noted that there was still no in situ characterization of an assembly process for MOFs on the molecular level.[10] In this assembly process two subunits have to be combined, organic ligands and metal precursors. Whereas the organic ligands are supplied directly as a reactant, the inorganic coupling units, also referred to as secondary building units (SBUs), have to be formed in the synthesis process from the metal precursors. The formation of the SBUs appears to be crucial for the MOF assembly process.[2]

Direct evidence for the participation and persistence of discrete SBUs during the MOF growth process was presented by Férey et al. with a detailed EXAFS study of the formation of MIL-89, $[Fe_3O(CH_3OH)_3\{O_2C(CH)_4CO_2\}_3]Cl{\cdot}6\,CH_3OH$ by starting with trinuclear basic iron(III) acetate as the precursor to the SBU and *trans*,*trans*-muconic acid as linker.[11] With similar motivation, Henderson et al. used electrospray ionization mass spectrometry (ESI) to monitor metal carboxylate nucleation in the case of the reaction of $Mg(NO_3)_2{\cdot}6\,H_2O$ with (+)-camphoric acid (H_2cam) in acetonitrile.[12] Soluble, dimetallic $[Mg_2(Hcam)_3]^+$ ions were found as key intermediates.

These studies were carried out in solution, thus growth occurs along all growth directions simultaneously and it is impossible to correlate kinetic studies with morphological results. It is also difficult to study the importance of the reactants individually since MOF growth occurs from a mixture containing a variety of species, reactants and intermediates, such as SBUs and possibly larger units. For these reasons it would be highly desirable to study the growth of a particular MOF along different crystallographic directions separately and to vary the metal precursor during the growth to elucidate the importance of the SBU.

One possibility to achieve such a goal would be to start from a MOF single crystal and to investigate the growth on the differently oriented surfaces of this substrate, in analogy to the homoepitaxial grow of simpler solids, for example, metals and semiconductors at the gas–solid interface.[13] In case of MOFs, of course, growth needs to be studied at the solid–liquid interface.[14]

Although using MOF single crystals for growth studies is in principle possible,[15] this is a rather difficult approach since the handling of the micrometer-sized single crystals is experimentally challenging. To date studies in ultrahigh vacuum (UHV) using atomic force microscopy (AFM) have been reported,[16] but it will be difficult to achieve such high resolution in a liquid. Herein, we present results obtained using a different approach. In a first step we grow highly ordered, oriented MOF layers, denoted as SURMOF (surface-mounted MOFs), using a step-by-step approach at mild conditions (i.e. room temperature) on templates (Scheme 1). The templates are different types of well-defined organic surfaces, which can be conveniently prepared by fabricating self-assembled monolayers (SAMs) on gold substrates.[17]

This growth method differs substantially from the conventional solvothermal synthesis of MOFs with homogeneous mixing of all the reactants (primary building blocks, typically two) at elevated temperatures between 70 and 150 °C.[1,4,18] Although the low temperature will substantially slow down the kinetics, the sequential contact with the separated reactants leads to a robust MOF layer with a well-defined thickness for each single step.[19] After completion of the first

[*] Dr. O. Shekhah, H. Wang, Prof. C. Wöll
Physical Chemistry I, Ruhr University Bochum
Universitätsstrasse 150, 44801 Bochum (Germany)
Fax: (+49) 234-322-4219
E-mail: woell@pc.rub.de
Homepage: http://www.pc.rub.de
D. Zacher, Prof. R. A. Fischer
Inorganic chemistry II, Ruhr University Bochum
Universitätsstrasse 150, 44801 Bochum (Germany)

[**] This was supported by the Priority Program 1362 "Metal-Organic Frameworks" of the German Research Foundation.

Supporting information for this article is available on the WWW under http://dx.doi.org/10.1002/anie.200900378.

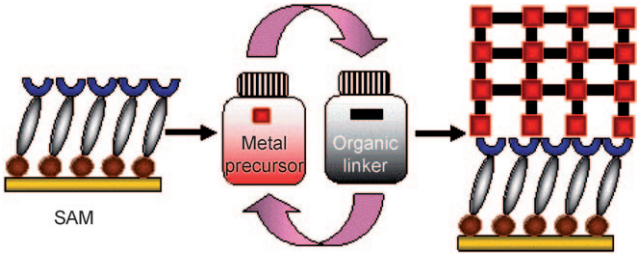

Scheme 1. The step-by-step approach for the growth of the SURMOFs on a SAM-functionalized substrate. The approach involves repeated cycles of immersion in solutions of the metal precursor and solutions of organic ligand. Between steps the material is rinsed with solvent.

deposited layer further growth proceeds as a MOF-on-MOF homoepitaxy. This growth mode is related to the recently reported heteroepitaxial growth of free-standing MOF core–shell microcrystallites.[15] As, in our case, the reactants are kept separate, mechanistic studies are possible and in particular it is feasible to vary the metal precursor during a deposition, thus allowing the relevance of the "controlled SBU approach" for MOF synthesis emphasized by Férey et al.[2,11] to be directly studied.

We present the potential of this concept for the case of $[Cu_3(btc)_2]$ (HKUST-1; $H_3btc = 1,3,5$-benzenetricarboxylic acid).[20] The deposition rate can be determined using surface plasmon resonance (SPR) spectroscopy,[19,21] and at any point the structure of the deposited MOF can be determined using X-ray diffraction (XRD). Figure 1 shows SPR data recorded during the deposition of $[Cu_3(btc)_2]$ SURMOFs using copper(II) acetate ($Cu(OAc)_2$) as a metallic precursor, on COOH and an OH-terminated SAMs, which were fabricated from 16-mercaptohexadecanoic acid (MHDA) and 11-mercaptoundecanol (MUD), respectively. An inspection of the growth curves reveals that the time constant for the deposition of the organic building block, H_3btc, is quite similar to that seen for the metal ions (Cu^{2+}) delivered from the $Cu(OAc)_2$. As the crucial step in both surface processes is the exchange reaction of the acetate (OAc^-) with the benzenetricarboxylate (btc^{3-}), the similar growth rates upon the cyclic exposure of the substrate to the two different components is not surprising.

We now turn to the question of the relevance of the metal-ion-containing component. In case of the usual synthesis method for $[Cu_3(btc)_2]$, copper(II) nitrate is used as a metal-ion precursor. Inspection of the bulk structure reveals that the growth of this MOF requires the formation of carboxylate-bridged paddle-wheel structured $(Cu^{2+})_2$ dimers (see Figure 2). The formation of these SBUs under solvothermal synthesis conditions has been proposed to be critical for the assembly of the MOF structure.[22] In our layer-by-layer growth experiment we can change the metal precursors in a straightforward fashion.

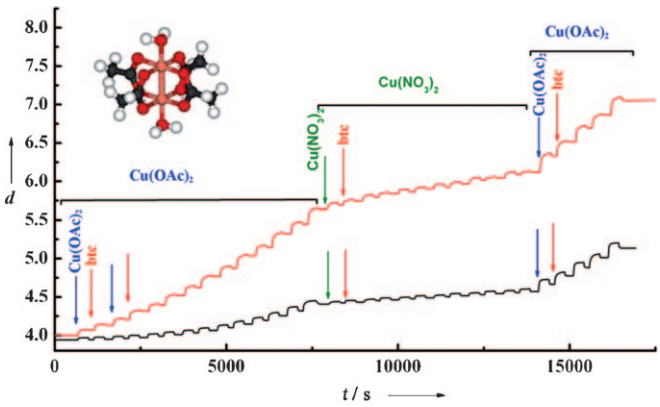

Figure 1. SPR signal as a function of time recorded in situ during the step-wise treatment of a MHDA SAM (red) and a MUD SAM (black) with $Cu(OAc)_2$, H_3btc, and $Cu(NO_3)_2$. Top left: molecular structure of copper(II) acetate hydrate $[Cu_2(CH_3COO)_4(H_2O)_2]$ as found in the solid state and in $Cu(OAc)_2$ solution. *d*: SURMOF thickness in 10^{-2} RIU (RIU: refractive index unit).[24]

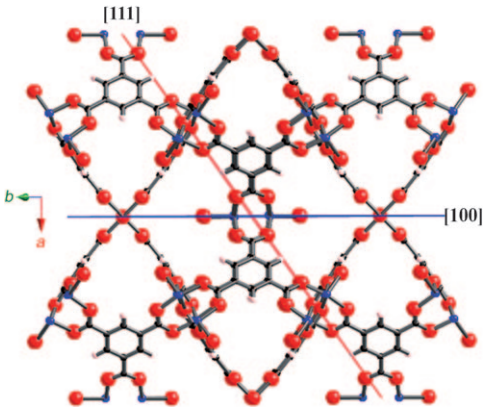

Figure 2. A side view of the unit cell of the hydrated $[Cu_3(btc)_2(H_2O)_3]$ (HKUST-1) where both planes [100] (blue line) and the [111] plane (red line) are shown. C gray, O red, Cu blue.

The data shown in Figure 1 reveal that virtually no deposition of MOF is observed on a MOF substrate when using copper nitrate as a precursor. At first sight this is surprising, because a similar exchange of the Cu^{2+} ion sources does not affect the MOF synthesis under solvothermal conditions, at all. If, after several cycles involving exposure to copper nitrate, the substrate is exposed to copper acetate again, a very regular growth is observed (Figure 1) with rates undistinguishable from those seen before switching to the copper nitrate. This finding can be rationalized by considering that in solutions of copper acetate the dominant unit present is the acetate-bridged paddle wheel $[Cu_2(CH_3COO)_4(H_2O)_2]$ (see inset in Figure 1).[23] This is important, since the $[Cu_3(btc)_2]$ framework is composed of very similar, btc-bridged Cu^{2+} dimers (Figure 2). In contrast, the structural chemistry of solvated copper(II) nitrate compounds is rather diverse,[20,21] but nitrate-bridged dinuclear paddle-wheel species have never been reported, neither in the solid state nor in solution. A monomeric form of anhydrous $Cu(NO_3)_2$ exists in the gas phase and as well in organic solvents with two nitrate ligands chelating the Cu^{2+} ion in a square-planar arrangement. Several polymeric modifications with bridging nitrate ions are known in the solid-state.[20] However, in a diluted ethanol solution of hydrated $Cu(NO_3)_2 \cdot 3H_2O$ (1 mM), as used for the SURMOF synthesis, the most abundant Cu^{2+} species is likely to be a mononuclear tetragonal stretched quasi-octahedral complex (Jahn–Teller distortion) with ethanol and/or water molecules coordinating at the equatorial plane and the substitution-labile monodentate nitrate ligands at the apical positions.[21]

Clearly, at the continuous-flow conditions of the layer-by-layer growth experiment these mononuclear species adsorb much less efficiently to a btc-terminated surface than the preformed dimeric SBU-like unit $[Cu_2(CH_3COO)_4(H_2O)_2]$ does. Consequently, the growth is significantly delayed when copper nitrate is used or related mononuclear Cu^{II} salts with other weakly coordinating counterions (e.g. ClO_4^-). With copper acetate as the Cu^{2+} source, one or two CH_3COO^- ligands of the dinuclear species (Figure 1) are displaced by the free carboxylate units of the btc groups, which are exposed at the [100] surfaces of the $[Cu_3(btc)_2]$ SURMOF (Figure 2).

This simple ligand-exchange reaction allows the anchoring of a preformed SBU at the growing surface and the formation of a monolayer of adsorbed SBUs, most likely terminated by acetate groups. This process is clearly entropically favored in comparison to chemisorption of the mononuclear Cu^{2+} species delivered by copper nitrate. It is instructive to closely study Figure 1 again, which clearly corroborates this mechanistic hypothesis: After exposure to several cycles of copper nitrate dosing without any substantial gain in thickness, exposure to copper acetate at once leads to a continuation of the MOF growth with an increase in thickness corresponding to half a unit cell along the [100] direction.[25]

In order to further investigate the general importance of preformed SBUs for the growth of $[Cu_3(btc)_2]$ crystallites it is necessary to study the growth along other crystallographic directions as well. Whereas monitoring deposition rates on different faces of MOF crystals is virtually impossible for other in situ growth studies of MOFs carried out recently in solution, for example, using light scattering,[26] electrospray ionization mass spectroscopy experiments,[12] or EXAFS,[11] the step-by-step approach in principle offers the possibility to set up such detailed experiments provided that very homogenous SURMOFs can be grown in different orientations on suitable substrates. The most promising strategy to obtain such a growth in a different direction is to use a different template for the liquid-phase epitaxy (Scheme 1). Considering the high density of OH groups along the [111] planes in the hydrated bulk structure of $[Cu_3(btc)_2(H_2O)_3]$ (Figure 2) we have chosen a OH-terminated organic surface (a SAM from MUD) to initiate growth. The XRD data shown in Figure 3 clearly demonstrates the success of this strategy. Whereas on a COOH-functionalized the growth of $[Cu_3(btc)_2]$ proceeds along the [100] direction, on a OH-terminated surface MOF-layers with a [111] orientation are grown.[19] Thus the organic surface not only nucleates the MOF growth but also controls the growth direction. In this context we emphasize that Bein et al.[27] observed the same orientation preference in their crystallization studies of MOFs. In their studies, organothiol-based COOH-terminated and OH-terminated SAMs were immersed at room temperature into an aged (8 days) and filtered mother solution for the solvothermal synthesis of HKUST-1 and MIL-88b.[27,28]

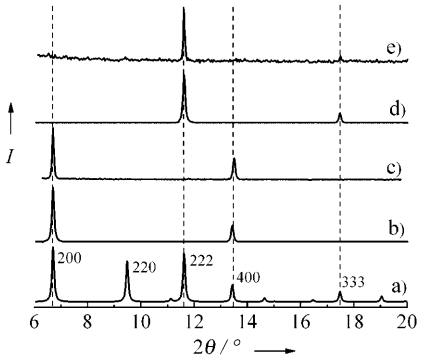

Figure 3. Out-of-plane XRD data for $[Cu_3(btc)_2(H_2O)_3]$. a) Powder, b) growth on a MHDA SAM (calculated), c) growth on MHDA SAM (experimental), d) growth on MUD SAM (calculated), e) grown on MUD SAM (experimental).

This template-effect of the organic surface can be rationalized by inspection of the bulk structure of $[Cu_3(btc)_2]$ (Figure 2). The preference for particular orientations can be predicted by bringing MOF single crystals with different surface orientation into contact with a particular organic surface and then estimating the interaction energy. A [100] plane can be chosen such that the resulting surface is terminated by metal-binding btc units only. Similarly, a [111] surface of $[Cu_3(btc)_2]$ will lead to the formation of copper–carboxylate bonds just as in the bulk phase. Differently oriented $[Cu_3(btc)_2]$ surfaces will contain both carboxylate-binding and Cu^{2+}-binding units, and therefore the interaction energy with a COOH-terminated surface will be substantially smaller.

It is therefore highly plausible that the quasi-epitaxial growth of $[Cu_3(btc)_2]$ on a COOH-terminated surface starts with the formation of [100] layer and then also proceeds in this direction. Understanding the oriented growth on OH-terminated surfaces requires a more refined analysis. During synthesis from ethanol/water solutions, H_2O molecules are coordinated to the Cu^{2+} ions of the SBUs in the apical positions (Figure 1). In the bulk phase the plane containing the highest density of these H_2O ligands is the [111] plane (see Figure 2). Therefore, a [111] oriented surface terminated by the H_2O ligands on the Cu^{2+} sites will show the highest stabilization energy upon contact with an OH-terminated surface among the different possible $[Cu_3(btc)_2]$ surface orientations. This reasoning explains the other orientation on the OH-terminated surface.[27]

The availability of a differently oriented MOF surface makes it possible to study the dependence of the MOF deposition rate on the surface termination of the substrate. Figure 1 reveals that the deposition rate on the OH-terminated organic surface is somewhat delayed and also the maximum growth rate under steady-state conditions is about half that on the [100] oriented surface. This result demonstrates that for different MOF surface terminations different growth rates are to be expected. Note, that a related tuning of the surface coordination chemistry should allow a targeted anisotropic growth of MOF (nano)crystals. Despite the substantial variation of the growth rates for the two different crystallographic orientations, again no growth is seen for copper nitrate on the [111] surface. As expected the observed SURMOF growth rate is constant over time for both orientations. However, a non-linear growth mode with a self-propagating behavior was recently reported for a related layer-by-layer synthesis of certain coordination polymers. Van der Boom et al. describe this effect for a surface coordination polymer (SCP) prepared from a polypyridyl osmium(II) complex and a palladium(II) precursor for cross linking the osmium units:[29] Although the structural properties and orientation of this particular SCP are less well defined than for SURMOFs, we anticipate that more complex, non-linear growth mechanisms of MOFs are possible.

In our related studies on liquid epitaxy of MILs using the controlled SBU approach, a promising growth behavior similar to that of $[Cu_3(btc)_2]$ was observed for the combination of $[Fe_3(O)(CH_3COO)_6(H_2O)_3]NO_3$ and btc. This system warrants further investigation so as to obtain an oriented film of MIL-100(Fe)[30] (see Supporting Information).

The in situ SPR monitoring of the step-by-step formation of MOFs allows novel mechanistic studies of the nucleation and growth of MOFs and the formation of the SBUs to be performed by investigating the deposition of the chosen building blocks separately. It also makes it possible to study growth rates as a function of crystallographic orientation. Our case study on HKUST-1 revealed significant differences along the [100] and the [111] direction, these differences are expected to become more pronounced for layer-based MOFs, such as $[Zn_2(bdc)L]$ (L = 1,4-diazabicyclo[2.2.2]octane or 4,4′-bipyridine). Most notably, the step-by-step approach offers a convenient method to study the effect of using chemically different metal-ion sources as precursors for the SBU and will enable a more systematic search for new reactants for the preparation of metal–organic frameworks.

Experimental Section

The $[Cu_3(btc)_2]$ (HKUST-1) materials were grown on gold substrates that were first functionalized by SAMs of 16-mercaptohexadecanoic acid (MHDA),[31,32] and 11-mercaptounodecanol (MUD). These functionalized substrates were then alternately immersed in a 1 mM ethanol solution of $Cu(CH_3COO)_2{\cdot}H_2O$ for 30 min and a 0.1 mM of benzenetricarboxylic acid (H_3btc) ethanol solution for 1 hour at room temperature. Between each step the substrates were rinsed with ethanol and dried in a stream of nitrogen gas. For infrared reflection-absorption spectroscopy (IRRAS), X-ray diffraction (XRD), and scanning electron microscope (SEM) measurements, polycrystalline Au substrates were prepared by evaporating a 5 nm buffer layer of titanium (99.8%, Chempur) and subsequently 100 nm of gold (99.995%, Chempur) onto polished silicon wafers (Wacker Siltronic) at room temperature in an evaporation chamber operating at a base pressure of about 10^{-7} mbar. For surface plasmon resonance (SPR) measurements, D263 thin glass (Schott) were rinsed with absolute ethanol, dried in a nitrogen stream, and then installed in a Leybold Inficon XTC/2 metal evaporator. Gold was evaporated onto a 12 Å buffer layer of titanium to reach a final thickness close to 485 Å. Evaporation was performed at room temperature under a pressure of approximately 10^{-7} mbar. IRRAS data were recorded using a Biorad Excalibur FTIR spectrometer (FTS 3000) equipped with a grazing incidence reflection unit (Biorad Uniflex) and a narrow band MCT detector. All spectra were recorded with 2 cm^{-1} resolution at an angle of incidence of 80° relative to the surface normal and further processed by using boxcar apodization. A commercial surface plasmon resonance system (Reichert SR7000DC) was used to record the real-time kinetics of the copper acetate, copper nitrate, and btc ligand adsorption to the both of the MHDA and the MUD organic surfaces. For the SPR experiments a 1 mM ethanol solution of $Cu(OAc)_2$, a 1 mM ethanol solution of $Cu(NO_3)_2{\cdot}3H_2O$, and 0.1 mM ethanol solution of H_3btc were used. X-ray diffraction (XRD) data for out-of-plane conditions were measured using a synchrotron radiation source (DELTA, Dortmund).

Received: January 20, 2009
Revised: April 1, 2009
Published online: June 2, 2009

Keywords: mechanistic studies · metal–organic frameworks · monolayers · nucleation · secondary building blocks

[1] J. Rowsell, O. Yaghi, *Microporous Mesoporous Mater.* **2004**, *73*, 3–14.
[2] G. Férey, *Chem. Mater.* **2001**, *13*, 3084–3098.
[3] B. F. Hoskins, R. Robson, *J. Am. Chem. Soc.* **1990**, *112*, 1546–1554.
[4] S. Kitagawa, R. Kitaura, S. Noro, *Angew. Chem.* **2004**, *116*, 2388–2430; *Angew. Chem. Int. Ed.* **2004**, *43*, 2334–2375.
[5] U. Mueller, M. Schubert, F. Teich, H. Puetter, K. Schierle-Arndt, J. Pastre, *J. Mater. Chem.* **2006**, *16*, 626–636.
[6] S. Bauer, N. Stock, *Chem. Unserer Zeit* **2008**, *42*, 12–19.
[7] S. Hermes, F. Schröder, R. Chelmowski, C. Wöll, R. A. Fischer, *J. Am. Chem. Soc.* **2005**, *127*, 13744–13745.
[8] S. Hermes, F. Schröder, S. Amirjalayer, R. Schmid, R. A. Fischer, *J. Mater. Chem.* **2006**, *16*, 2464–2472.
[9] S. Hermes, F. Schröder, R. Schmid, L. Khodeir, M. Muhler, A. Tissler, R. W. Fischer, R. A. Fischer, *Angew. Chem.* **2005**, *117*, 6394–6397; *Angew. Chem. Int. Ed.* **2005**, *44*, 6237–6241.
[10] A. K. Cheetham, C. N. R. Rao, R. K. Feller, *Chem. Commun.* **2006**, 4780–4795.
[11] S. Surblé, F. Millange, C. Serre, G. Férey, R. I. Walton, *Chem. Commun.* **2006**, 1518–1520.
[12] J. A. Rood, W. C. Boggess, B. C. Noll, K. W. Henderson, *J. Am. Chem. Soc.* **2007**, *129*, 13675–13682.
[13] T. Michely, J. Krug, *Islands, Mounds and Atoms: Patterns and Processes in Crystal Growth Far from Equilibrium*, Springer, Heidelberg, 1st ed., **2003**.
[14] K. Szelagowska-Kunstman, P. Cyganik, M. Goryl, D. Zacher, Z. Puterova, R. A. Fischer, M. Szymonski, *J. Am. Chem. Soc.* **2008**, *130*, 14446–14447.
[15] S. Furukawa, K. Hirai, K. Nakagawa, Y. Takashima, R. Matsuda, T. Tsuruoka, M. Kondo, R. Haruki, D. Tanaka, H. Sakamoto, S. Shimomura, O. Sakata, S. Kitagawa, *Angew. Chem.* **2009**, *121*, 1798–1802; *Angew. Chem. Int. Ed.* **2009**, *48*, 1766–1770.
[16] K. Szelagowska-Kunstman, P. Cyganik, M. Goryl, D. Zacher, Z. Puterova, R. A. Fischer, M. Szymonski, *J. Am. Chem. Soc.* **2008**, *130*, 14446–14447.
[17] L. E. J. Love, J. Kriebel, R. Nuzzo, G. Whitesides, *Chem. Rev.* **2005**, *105*, 1103–1169.
[18] D. Zacher, O. Shekhah, C. Wöll, R. A. Fischer, *Chem. Soc. Rev.* **2009**, DOI: 10.1039/b805038b.
[19] O. Shekhah, H. Wang, S. Kowarik, F. Schreiber, M. Paulus, M. Tolan, C. Sternemann, F. Evers, D. Zacher, R. A. Fischer, C. Wöll, *J. Am. Chem. Soc.* **2007**, *129*, 15118–15119.
[20] D. J. Tranchemontagne, J. R. Hunt, O. M. Yaghi, *Tetrahedron* **2008**, *64*, 8553–8557.
[21] M. Mrksich, G. B. Sigal, G. M. Whitesides, *Langmuir* **1995**, *11*, 4383–4385.
[22] A. F. Wells, *Structural Inorganic Chemistry*, 5th ed., Clarendon Press, Oxford, **1995**.
[23] N. J. Manin, D. V. Baranov, V. P. Korolev, *Russ. J. Inorg. Chem.* **2003**, *48*, 288–293.
[24] J. N. Van Niekerk, F. R. L. Schoening, *Nature* **1953**, *171*, 36–37.
[25] C. Munuera, O. Shekhah, H. Wang, C. Wöll, C. Ocal, *Phys. Chem. Chem. Phys.* **2008**, *10*, 7257–7261.
[26] D. Zacher, J. Liu, K. Huber, R. A. Fischer, *Chem. Commun.* **2009**, 1031–1033.
[27] E. Biemmi, C. Scherb, T. Bein, *J. Am. Chem. Soc.* **2007**, *129*, 8054–8055.
[28] C. Scherb, A. Schödel, T. Bein, *Angew. Chem.* **2008**, *120*, 5861–5863; *Angew. Chem. Int. Ed.* **2008**, *47*, 5777–5779.
[29] L. Motiei, M. Altman, T. Gupta, F. Lupo, A. Gulino, G. Evmenenko, P. Dutta, M. E. van der Boom, *J. Am. Chem. Soc.* **2008**, *130*, 8913–8914.
[30] P. Horcajada, S. Surblé, C. Serre, D. Y. Hong, Y. K. Seo, J. S. Chang, J. M. Greneche, I. Margiolaki, G. Férey, *Chem. Commun.* **2007**, 2820–2822.
[31] R. Arnold, W. Azzam, A. Terfort, C. Wöll, *Langmuir* **2002**, *18*, 3980–3992.
[32] H. J. Himmel, A. Terfort, C. Wöll, *J. Am. Chem. Soc.* **1998**, *120*, 12069–12074.

